



Fouling of reverse osmosis membranes by cane molasses fermentation wastewater: detection by electrical impedance spectroscopy techniques

Jie Cen*, John Kavanagh, Hans Coster, Geoff Barton

*School of Chemical and Biomolecular Engineering, The University of Sydney, Sydney, Australia
Tel. +61 433315962; email: jie.cen@sydney.edu.au*

Received 1 March 2012; Accepted 18 July 2012

ABSTRACT

The electrical impedance as a function of frequency (electrical impedance spectroscopy [EIS]) of both clean and fouled reverse osmosis (RO) membranes was monitored under osmotic pressure-driven conditions to introduce a water flux through the membranes. RO membranes were fouled using a pilot-scale facility with cane molasses wastewater. Fouling was revealed via a diffusion polarization layer observed below 100 Hz. This fouling layer contained both reversible and irreversible parts. The fouling component that was irreversible contributed mainly to the EIS spectra in the frequency range of 0.01–0.1 Hz, while the reversible fouling component dominated in the range of 0.1–100 Hz. Results presented demonstrate that electrical impedance spectroscopy is able to quantitatively measure real foulants on the surface of RO membranes.

Keywords: Fouling; EIS; RO; Wastewater

1. Introduction

Fouling can significantly impact a membrane's operational lifetime and the permeate flux obtained [1], with severe fouling resulting in unscheduled shut-downs leading to a loss of productivity. Moreover, fouling leads to extra power consumption due to the need for higher pressures to maintain the flux [2]. Indeed, Bates [3] highlights that the economic viability of reverse osmosis (RO) systems is greatly dependent on membrane fouling. Even if fouling is successfully controlled, there are high costs associated with fouling control done either by pre-treatment or membrane

cleaning [4,5], which again can significantly reduce the economic potential of any operational RO system [6].

Common techniques used in previous studies for characterizing membrane and fouling layers mostly focus on the determination of their morphological, chemical and physical properties. These techniques include scanning electron microscopy (SEM), X-ray photoelectron spectroscopy (XPS) and atomic force microscopy (AFM). For example, Kim et al. [7–9] successfully applied these techniques to study the mechanisms of membrane fouling. Similarly, Dietz et al. [10] identified the structural differences between clean and fouled membrane based on AFM images. However, all these techniques involve cessation of the filtration process and the destruction of the membrane—essentially they are only useful as membrane autopsies. The tech-

*Corresponding author.

Presented at the International Conference on Desalination for the Environment, Clean Water and Energy, European Desalination Society, 23–26 April 2012, Barcelona, Spain

nique we are proposing is electrical impedance spectroscopy (EIS), which has been used as a non-invasive tool in a number of membrane systems [6,11–16]. In essence, the technique works by injecting a small alternating current (AC) of known frequencies into the system and measuring the voltage and phase difference between the current and voltage across the system. Impedance dispersion can then be used to distinguish different “layers” that comprise the system of interest including any fouling layers. A study by Park et al. [17] has shown the potential of EIS in real-time monitoring of fouling in ion-exchange membranes. Moreover, preliminary results obtained by Kavanagh et al. [18] have demonstrated its potential in RO systems.

Here we present a different approach that is similar to a membrane autopsy but using EIS, in which membranes are fouled for different durations of time in a commercial membrane separation module and then examined using EIS afterwards. A water flux was also established in the membrane EIS chamber during the measurements using solutions of different concentration on the two sides of the membrane. This paper thus aims to examine the feasibility of EIS to detect real foulants (from cane molasses fermentation wastewater) and to identify the difference in electrical properties of clean and fouled membranes. The limitations of the method, data analysis and associated experimental difficulties are discussed in detail.

2. Theory

Impedance measurements are made by injecting an AC of known frequency ω and small amplitude i_o into a membrane system and measuring the amplitude v_o and phase difference \varnothing of the concomitant electrical potential difference that develops across the sample under consideration

$$|Z| = \frac{v_o}{i_o} \quad \text{and} \quad \angle Z = \varnothing \quad (1)$$

The conductance G and the capacitance C describe the ability of the homogeneous material to conduct and store electric charge, respectively. The impedance measurement provides estimates of these parameters as follows:

$$G = \frac{1}{|Z|} \cos \varnothing \quad \text{and} \quad C = -\frac{1}{\omega|Z|} \sin \varnothing \quad (2)$$

For a uniform single slab of material with cross-sectional area A and thickness x , these properties are given by:

$$G = \sigma \frac{A}{x} \quad \text{and} \quad C = \varepsilon \frac{A}{x} \quad (3)$$

where the constants σ and ε are the electrical conductivity and dielectric permittivity of the material, respectively.

In membrane systems, the electric current is carried by ions that move by diffusion under the influence of concentration gradients as well as by electric fields. A diffusion polarization effect can result by an enhancement of electrically charged species in the unstirred surface layers on one side of the membrane and a depletion of these species in the corresponding layers on the opposite side [11]. As a result, a membrane system is generally composed of several layers with different properties and hence the capacitance and conductance will be frequency dependent. However, in this study, we will not discuss the membrane substructure in details as our main purpose is to detect fouling.

The electrical circuit model used in this study is assumed to comprise four/five elements as previously proposed by Kavanagh et al. [18] and illustrated in Fig. 1. This includes the following:

- An element to represent the membrane/bulk solution contact resistance (G_{sol});
- An element to represent the conductance (G_{diff}) and capacitance (C_{diff}) of the diffusion polarization layer;
- An element to represent the conductance (G_f) and capacitance (C_f) of the fouling layer (i.e. the dotted line element);
- An element to represent the conductance (G_{mem}) and capacitance (C_{mem}) of the membrane.

3. Materials and methods

3.1. Membrane and preparation

Polyamide RO membranes (Alfa Laval Ltd.) were used in this investigation. They were thin-film composite membranes designed for brackish water salt removal, with nominal rejection of >97%¹ and pH range 2–11. All membranes were pre-wetted by soaking in ethanol for an hour and then rinsed thoroughly in deionised water, before storing in deionised water for 24 h.

3.2. Foulants

Cane molasses fermentation wastewater was used as the fouling agent. They have a pH of 7.5, COD of 1,010 mg/L, conductivity of 5.7 mS cm⁻¹ at 24°C and DOC of 1,630 ppm.

¹Measured on 2,000 ppm NaCl, 16 bar, 25°C according to manufacturer’s instructions.

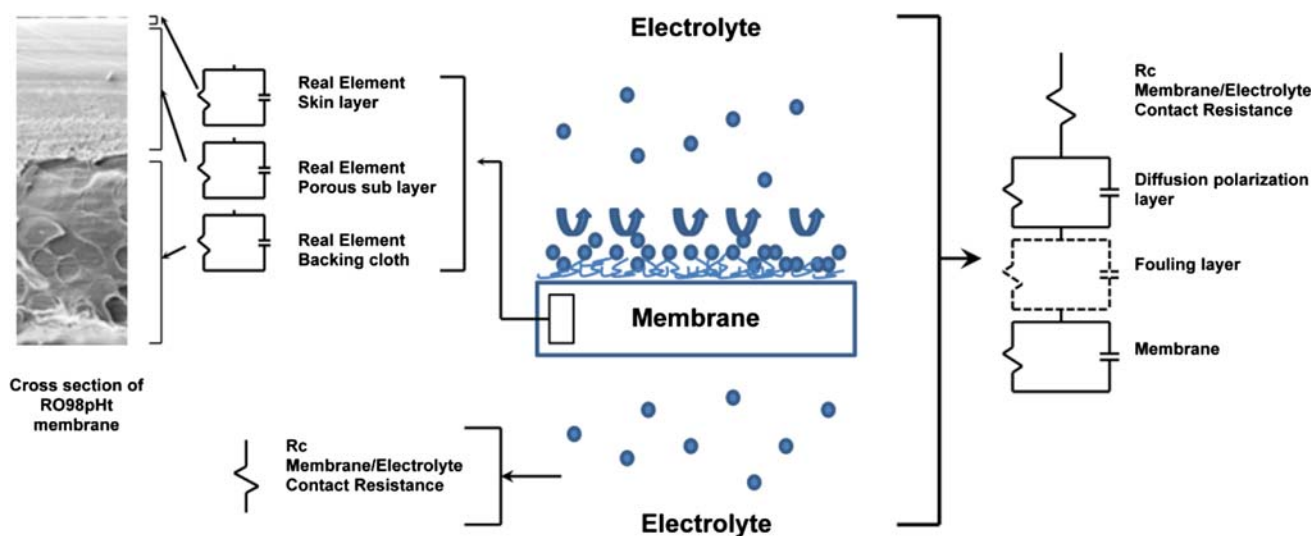


Fig. 1. The proposed circuit model.

The composition of cane molasses fermentation wastewater is complex, but the main foulants are humic substances, such as humic and fulvic acids [19,20] that form a cake-like layer on the surface of the membrane.

3.3. Experimental procedure

Fouling tests were conducted using a pilot-scale rig (Alfa Laval M16 module) to pre-foul the membranes using cane molasses fermentation wastewater. Experiments were commenced with the compaction of the membrane for 3 h using deionised water at an applied pressure of 30 bar, a temperature of $25 \pm 1^\circ\text{C}$ and at the desired cross-flow rate. Subsequently, the wastewater was introduced, following drainage of the deionised water. The operational permeate flow was measured using a flow transmitter (McMillan Model 107). The experimental runs are summarized as below:

- Membrane compacted for 3 h with no fouling as a “clean” control.
- Compacted for 3 h and fouled for 1 h.
- Compacted for 3 h and fouled for 3 h.
- Compacted for 3 h and fouled for 6 h.

Samples of the fouled membranes were cut and put into the four-terminal EIS chamber (Fig. 2(a)) to obtain electrical impedance spectra. Four impedance spectra were recorded, with each spectrum taken at 4 hourly intervals. The EIS measurements were done under osmotic pressure-driven conditions to introduce a water flux through membranes. The feed and draw solutions were 5 mM and 500 mM NaCl solutions,

respectively, with the membrane skin layer facing the lower concentration of solution. These solutions were re-circulated via a peristaltic pump with separate connections into the EIS chamber (Fig. 2(b)). Water flux was also recorded using a weighing balance.

4. Results and discussion

4.1. Effect of fouling

Fig. 3(a) shows a comparison of the capacitance vs. frequency between the compacted clean membrane and the membranes fouled for different durations. It can be seen that the difference mainly occurs below 100 Hz where the measured capacitance increased by several orders of magnitude with decreasing frequency. An exceptional curve below the frequency of 0.1 Hz was also observed for the system of compacted clean membrane. The drop in capacitance, to even negative values, between the frequency range 0.01–1 Hz probably resulted from the electro-osmotic effects arising from coupling between the ion flow and the water flux [21]. Fitting of the circuit model to the conductance and capacitance dispersion data indicates that below 100 Hz, we are seeing the impact of diffusion polarization at the surface of membrane. As a result, the effect of fouling was revealed via its impact in the diffusion polarization regime [11,15].

Furthermore, it was noted that the fouling effect on the EIS revealed two distinct results for the capacitance as a function of frequency. In one region (0.01–0.1 Hz) (Fig. 3(b)), the capacitance increased with increasing fouling time. In the other region (0.1–100 Hz) (Fig. 3(c)), capacitance decreased with increasing fouling time.

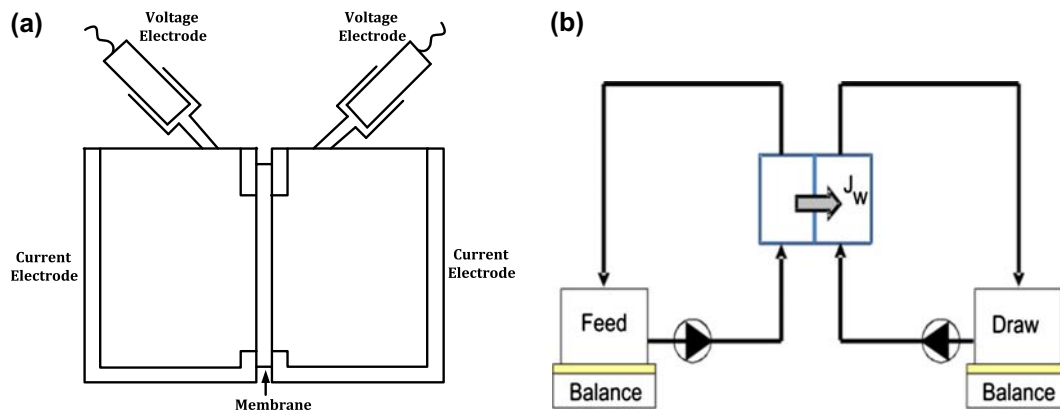


Fig. 2. Schematic representation of (a) four-terminal chamber used and (b) EIS measurement set-up.

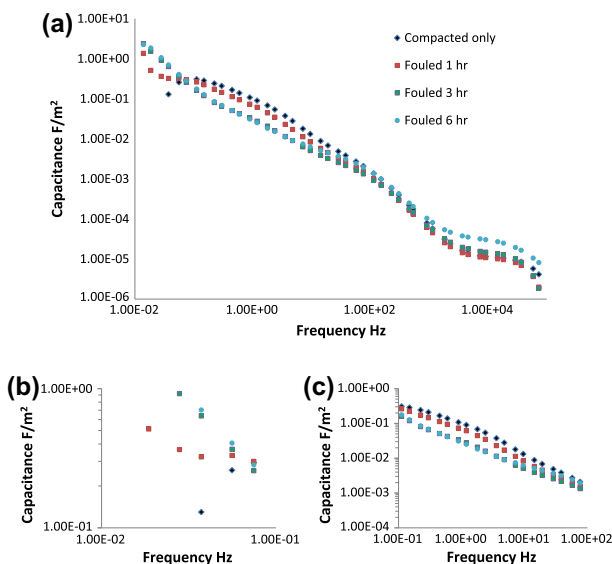


Fig. 3. (a) Comparison of the EIS for fouled membranes and a compacted clean membrane. A close-up in the frequency range of 0.01–0.1 Hz (b) and 0.1–100 Hz (c).

In Fig. 4, we compare the reduction in capacitance at a frequency of 1 Hz with the reduction in permeate flux, which is the most common fouling indicator. For the membrane fouled for 1 h, the reduction in capacitance was around 40%, while the permeate flux decline was only 20%. For 6 h of fouling, the capacitance at 1 Hz dropped by 71%, while the flux declined by 55% over the period. These figures indicate that EIS responses more sensitively to fouling than the permeate flux.

4.2. Loss of fouling layer

The photographs in Table 1 (left column) show that the RO membranes were fouled at the chosen operational conditions, and there was more fouling accumu-

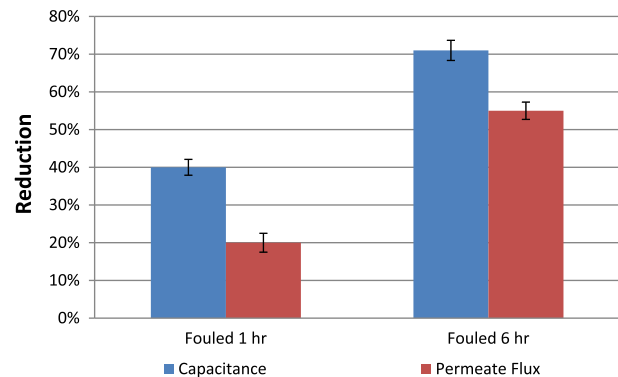










Fig. 4. Reduction in capacitance at a frequency of 1 Hz and permeate flux due to membrane fouling.

lation with increasing run time. However, a significant loss in the fouling layer occurred during subsequently repeated EIS measurements, as some of the cake became dislodged with time (see Table 1, right column). Although the salt solution circulating through the chamber had washed away most of the fouling layer by the end of the measurement, it was still possible to see some fouling residue left on the surface of the membrane even after 12 h. This suggests that the fouling layer may contain two parts. One part being a loose/thick layer that could be washed away easily by water, while the second part was compact and thin and could only be removed by a cleaning solution.

Similarly, differences were observed in EIS measurements taken at different times for membrane samples. Fig. 5(a) shows the four spectra for the membrane sample fouled for 6 h. The spectrum at the beginning of EIS measurements ($t=0$) appears to be quite different from the others, especially in the frequency range below 100 Hz. As discussed in the previous section, the fouling effect was mainly observed in that frequency range. Therefore, such differences

Table 1
The comparison between membrane samples at the beginning and the end of EIS measurement

	Beginning of EIS measurement ($t = 0$)	End of EIS measurement ($t = 12$ h)
Membrane compacted only		
Membrane compacted and fouled for 1 h		
Membrane compacted and fouled for 3 h		
Membrane compacted and fouled for 6 h		

are believed to be directly related to the dislodgement of the fouling layer (i.e. back into the solution). It is also illustrated in Fig. 5(b) where the spectra taken at $t = 4, 8$ and 12 h are similar to the spectrum for the compacted clean membrane expect at very low frequencies. It provides further evidence of EIS detection of the loss of the fouling layer. The same trend can be found in the EIS data for the other membrane sam-

ples. Nevertheless, there was almost no difference in capacitance response between the spectra taken at $t = 4, 8$ and 12 h for the membrane sample fouled for 6 h. Since the rate of loss of the cake layer was unknown, but it is quite likely that when measurement of the second spectrum started, the “reversible part” of the fouling layer had already been washed away.

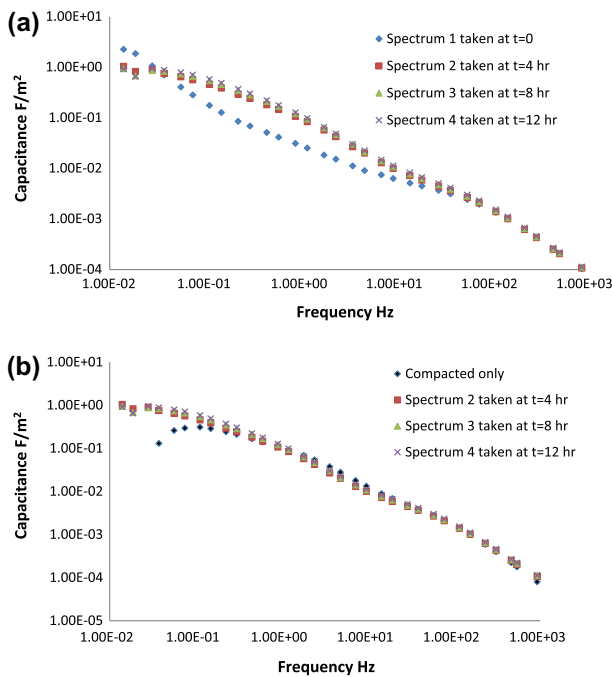


Fig. 5. (a) Comparison between four spectra taken at different durations for the membrane fouled for 6 h. (b) Comparison between the compacted clean membrane and the membrane fouled for 6 h taken at $t=4$, 8 and 12 h of EIS measurements.

4.3. Irreversible and reversible fouling components

Comparing the compacted clean membrane with the spectrum of the fouled membranes, which was taken at $t=12$ h EIS measurement (Fig. 6(a)), the difference in the frequency range of 0.1–100 Hz disappears, while the effect in the other region remains. As discussed previously, the difference between the spectra taken at $t=0$ and 12 h for the fouled membranes corresponds to the dislodgement of the reversible part of the fouling cake. Thus, it is reasonable to conclude that the irreversible and reversible parts of the fouling layer affect the impedance spectra in the frequency ranges 0.01–0.1 Hz and 0.1–100 Hz, respectively.

We noted that capacitance decreased with increasing fouling time between 0.1 and 100 Hz. This implies Eq (4) that there was an increase in the thickness of the layer. Thus, in the range 0.1–100 Hz, the reversible part of the fouling layer had dominated over any diffusion polarization effect. On the other hand, we see (Fig. 6(b)) that the drop in capacitance caused by electro-osmotic effects, which showed up in the frequency range 0.01–0.1 Hz, disappeared with longer fouling times. This suggested that additional irreversible fouling (produced by longer fouling time) had hindered water diffusion through the membrane and enhanced

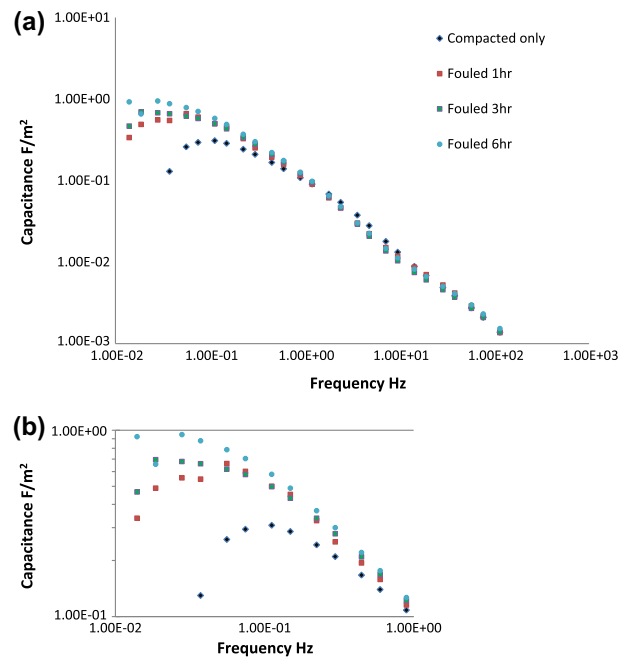


Fig. 6. Comparison between fouled membranes and the compacted clean membrane at $t=12$ h of EIS measurements. (a) Capacitance behaviour in the frequency range of 0.01–100 Hz. (b) A close-up for the frequency range of 0.01–1 Hz.

the diffusion polarization effect, which then masks the electro-osmotic effects.

5. Conclusions

This paper has demonstrated that EIS has potential for measuring real foulants on the surface of RO membranes.

It is concluded that the fouling effect was revealed by an enhanced diffusion polarization layer at frequencies below 100 Hz rather than in the formation of an extra layer. It is also found that the fouling layer contained a reversible and an irreversible fouling part. The irreversible fouling mainly contributed to changes in capacitance in the frequency range of 0.01–0.1 Hz, while the reversible fouling mainly contributed in the frequency range of 0.1–100 Hz. The reduction in capacitance associated with the reduction in permeate flux due to fouling indicates that the EIS responses are more sensitive to fouling than the permeate flux. The loss of the fouling layer was observed during EIS measurement over time. However, such losses also showed up in impedance data for each fouled membrane.

Since the loss rate of the fouling layer was not known, we could not quantitatively relate the cake layer of fouling to the impedance response. Further

electrical impedance measurements need to focus on using in situ fouling measurement, in which the EIS data are measured during the fouling process.

Acknowledgements

The authors gratefully acknowledge financial support via *ARC Linkage Project LP100100310: Measurement and Prevention of Membrane Fouling for Water Reuse in Biorefineries and the Endeavour International Postgraduate Research Scholarship*. They would also like to thank Milan Vukas for his assistance on some of the fouling experiments and the AMMRF (Australian Microscopy and Microanalysis Research Facility) for their SEM images.

References

- [1] T.b.M.A. Al Sajwani, The desalination plants of Oman: Past, present and future, *Desalination* 120 (1998) 53–59.
- [2] K.G. Tay, L. Song, A more effective method for fouling characterization in a full-scale reverse osmosis process, *Desalination* 177 (2005) 95–107.
- [3] W.T. Bates, Reducing the fouling rate of surface and waste water RO systems, in: *The International Water Conference, USA, 1998*, pp. 59–65.
- [4] H. Mo, K.G. Tay, H.Y. Ng, Fouling of reverse osmosis membrane by protein (BSA): Effects of pH, calcium, magnesium, ionic strength and temperature, *J. Membr. Sci.* 315 (2008) 28–35.
- [5] K. Scott, *Handbook of Industrial Membranes*, first ed., Elsevier Advanced Technology, Oxford, 1995.
- [6] H.G.L. Coster, K.J. Kim, K. Dahlan, J.R. Smith, C.J.D. Fell, Characterisation of ultrafiltration membranes by impedance spectroscopy. I. Determination of the separate electrical parameters and porosity of the skin and sublayers, *J. Membr. Sci.* 66 (1992) 19–26.
- [7] K.J. Kim, V. Chen, A.G. Fane, Characterization of clean and fouled membranes using metal colloids, *J. Membr. Sci.* 88 (1994) 93–101.
- [8] K.-J. Kim, V. Chen, A.G. Fane, Ultrafiltration of colloidal silver particles: Flux, rejection, and fouling, *J. Colloid Interface Sci.* 155 (1993) 347–359.
- [9] K.-J. Kim, A.G. Fane, Low voltage scanning electron microscopy in membrane research, *J. Membr. Sci.* 88 (1994) 103–114.
- [10] P. Dietz, P.K. Hansma, O. Inacker, H.-D. Lehmann, K.-H. Herrmann, Surface pore structures of micro- and ultrafiltration membranes imaged with the atomic force microscope, *J. Membr. Sci.* 65 (1992) 101–111.
- [11] H.G.L. Coster, T.C. Chilcott, A.C.F. Coster, Impedance spectroscopy of interfaces, membranes and ultrastructures, *Bioelectrochem. Bioenerg.* 40 (1996) 79–98.
- [12] L. Gaedt, T.C. Chilcott, M. Chan, T. Nantawisarakul, A.G. Fane, H.G.L. Coster, Electrical impedance spectroscopy characterisation of conducting membranes: II. Experimental, *J. Membr. Sci.* 195 (2002) 169–180.
- [13] H.-T. Kim, J.-K. Park, K.-H. Lee, Impedance spectroscopic study on ionic transport in a pH sensitive membrane, *J. Membr. Sci.* 115 (1996) 207–215.
- [14] T. Hanai, K. Zhao, K. Asaka, K. Asami, Dielectric theory of concentration polarization. Relaxation of capacitance and conductance for electrolyte solutions with locally varying conductivity, *J. Membr. Sci.* 64 (1991) 153–161.
- [15] K. Zhao, M. Yasuhiro, K. Asaka, K. Asami, T. Hanai, Dielectric analysis of concentration polarization phenomena at cation-exchange membrane/solution interfaces by frequency variation and d.c. bias application, *J. Membr. Sci.* 64 (1991) 163–172.
- [16] E. James Watkins, P.H. Pfromm, Capacitance spectroscopy to characterize organic fouling of electro dialysis membranes, *J. Membr. Sci.* 162 (1999) 213–218.
- [17] J.S. Park, T.C. Chilcott, H.G.L. Coster, S.H. Moon, Characterization of BSA-fouling of ion-exchange membrane systems using a subtraction technique for lumped data, *J. Membr. Sci.* 246 (2005) 137–144.
- [18] J.M. Kavanagh, S. Hussain, T.C. Chilcott, H.G.L. Coster, Fouling of reverse osmosis membranes using electrical impedance spectroscopy: Measurements and simulations, *Desalination* 236 (2009) 187–193.
- [19] T. Handelsman, T. Nguyen, M. Vukas, G. Barton, H. Coster, F. Roddick, J. Kavanagh, Characterisation of foulants in membrane filtration of biorefinery effluents, in: *Desalination for the Environment Clean Water and Energy, Barcelona, Spain, 2012*.
- [20] Y. Satyawali, M. Balakrishnan, Wastewater treatment in molasses-based alcohol distilleries for COD and color removal: A review, *J. Environ. Manage.* 86 (2008) 481–497.
- [21] H.G.L. Coster, T.C. Chilcott, The characterization of membranes and membrane surfaces using impedance spectroscopy, In: T.S. Sorensen (Ed), *Surface Chemistry and Electrochemistry of Membranes*, Marcel Dekker, New York, NY, 1999, pp. 749–792.